REPORT DOCUMENTATION PAGE

Form Approved
OMB No. 0704-0188

1. REPORT DATE *(DD-MM-YYYY)*	**2. REPORT TYPE**	**3. DATES COVERED** *(From - To)*
2016	Open Literature	

4. TITLE AND SUBTITLE
Identification and validation of vesicant therapeutic targets using a high. throughput siRNA screening approach

5a. CONTRACT NUMBER

5b. GRANT NUMBER

5c. PROGRAM ELEMENT NUMBER

6. AUTHOR(S)
Ruff, AL, Beach, S, Lehman, J, Rothwell, C, Dillman, JF III

5d. PROJECT NUMBER

5e. TASK NUMBER

5f. WORK UNIT NUMBER

7. PERFORMING ORGANIZATION NAME(S) AND ADDRESS(ES)

US Army Medical Research Institute of Chemical Defense
ATTN: MCMR-CDR-C
3100 Ricketts Point Road
Aberdeen Proving Ground, MD 21010-5400

8. PERFORMING ORGANIZATION REPORT NUMBER

USAMRICD-P14-011

9. SPONSORING / MONITORING AGENCY NAME(S) AND ADDRESS(ES)
Defense Threat Reduction Agency
8725 John J. Kingman Road STOP 6201
Fort Belvoir, VA 22060-6201

10. SPONSOR/MONITOR'S ACRONYM(S)

11. SPONSOR/MONITOR'S REPORT NUMBER(S)

12. DISTRIBUTION / AVAILABILITY STATEMENT

Approved for public release; distribution unlimited

13. SUPPLEMENTARY NOTES
Published in Archives of Toxicology, 90:375–383, 2016. This research was supported by the Defense Threat Reduction Agency—Joint Science and Technology Office, Medical S&T Division, Project ID Number CBM.CUTOC.04.10.

14. ABSTRACT
See reprint.

15. SUBJECT TERMS
sulfur mustard, cutaneous injury, siRNA, high-throughput screening, inflammation, in vitro models

16. SECURITY CLASSIFICATION OF:			**17. LIMITATION OF ABSTRACT**	**18. NUMBER OF PAGES**	**19a. NAME OF RESPONSIBLE PERSON**
a. REPORT	**b. ABSTRACT**	**c. THIS PAGE**			Albert L. Ruff
UNCLASSIFIED	UNCLASSIFIED	UNCLASSIFIED	UNLIMITED	9	**19b. TELEPHONE NUMBER** *(include area code)* 410-436-8456

Arch Toxicol (2016) 90:375–383
DOI 10.1007/s00204-014-1427-z

ORGAN TOXICITY AND MECHANISMS

Identification and validation of vesicant therapeutic targets using a high-throughput siRNA screening approach

Albert L. Ruff · Sarah Beach · John Lehman · Cristin Rothwell · James F. Dillman

Received: 15 September 2014 / Accepted: 25 November 2014 / Published online: 24 December 2014

Abstract Sulfur mustard [SM, bis-(2-chloroethyl) sulfide] is a highly reactive bifunctional alkylating agent that has been used as a vesicating agent in warfare scenarios to induce severe lung, skin, and eye injury. SM cutaneous lesions are characterized by both vesication and severe inflammation, but the molecular mechanisms that lead to these signs and symptoms are not well understood. There is a pressing need for effective therapeutics to treat this injury. An understanding of the molecular mechanisms of injury and identification of potential therapeutic targets is necessary for rational therapeutic development. We have applied a high-throughput small interfering RNA (siRNA) screening approach to the problem of SM cutaneous injury in an effort to meet these needs. Our siRNA screening efforts have initially focused on SM-induced inflammation in cutaneous injury since chronic inflammation after exposure appears to play a role in progressive clinical pathology, and intervention may improve clinical outcome. Also, targets that mitigate cellular injury should reduce the inflammatory response. Historical microarray data on this injury were mined for targets and pathways implicated in inflammation, and a siRNA library of 2,017 targets was assembled for screening. Primary screening and library deconvolution were performed using human HaCaT keratinocytes and focused on cell death and inflammatory markers as end points. Using this in vitro approach, we have identified and validated novel targets for the potential treatment of SM-induced cutaneous injury.

Keywords Sulfur mustard · Cutaneous injury · siRNA · High-throughput screening · Inflammation · In vitro models

Introduction

Sulfur mustard (SM, bis-(2-chloroethyl) sulfide) is a highly reactive bifunctional alkylating agent and has been used in warfare scenarios as a potent vesicating agent to induce severe lung, skin, and eye injury (for a review, see Papirmeister et al. 1991). SM covalently modifies DNA, proteins, and other macromolecules (Deaton et al. 1990; Dillman et al. 2003; Langenberg et al. 1998; Papirmeister et al. 1991). DNA damage has long been hypothesized to play a primary role in the cellular response to SM exposure (Fox and Scott 1980; Herriott and Price 1948; Lawley and Brookes 1965, 1968; Papirmeister et al. 1969); however, the contribution of other alkylation events to the response remains largely unknown. Clinically, SM cutaneous lesions are characterized by both vesication and severe inflammation (Papirmeister et al. 1991). The molecular mechanisms that lead to these signs and symptoms are not well understood. Microarray studies have shown that several molecular pathways are activated in response to SM exposure (Dillman et al. 2006; Rogers et al. 2004; Sabourin et al. 2004). These can be categorized broadly into inflammatory and apoptotic/necrotic pathways. Several other studies have implicated a number of different pathways and signaling molecules such as p53, p38α MAPK, and caspases just to

Disclaimer: The views expressed in this article are those of the author(s) and do not reflect the official policy of the Department of Army, Department of Defense, or the US Government.

A. L. Ruff (✉) · S. Beach · J. Lehman · C. Rothwell · J. F. Dillman
Cell and Molecular Biology Branch, Research Division, US Army Medical Research Institute of Chemical Defense, 3100 Ricketts Point Road, Aberdeen Proving Ground, MD 21010-5400, USA
e-mail: albert.l.ruff2.civ@mail.mil

name a few (for a review, see Kehe et al. 2009; Ruff and Dillman 2007). However, inhibitors of these targets have not been very successful in ameliorating the effects of SM exposure.

The molecular and cellular response to any disease or injury is typically complex; however, in many cases, these complexities often follow a relatively defined initiating mechanism. In the case of SM injury, even the initiating events are complex because SM reacts with numerous biological molecules. This myriad of other molecules alkylated by SM likely contributes to the clinical progression of injury despite the long-held hypothesis that SM DNA damage is the primary lesion leading to cell death. The regulatory pathways involved in response to SM are also complex and show interplay between major regulators of major biological pathways such as inflammation, cellular differentiation, and cell death. For example, using siRNA, our research group identified the MAPK p38α signaling pathway as a critical regulator of vesicant-induced inflammatory cytokine production (Ruff and Dillman 2010). However, p38 has also been shown to promote SM-induced keratinocyte terminal differentiation, a role that is negatively influenced by ERK1/2 activity (Popp et al. 2011). There is a pressing need to understand the molecular mechanisms of this injury and to identify potential therapeutic targets. Given the diversity of molecules that react with SM and the complexity of the regulatory pathways involved, traditional methods of pathway mapping are unlikely to meet these needs in a timely manner.

Our earlier work on the role of p38α in SM-induced inflammation demonstrated that siRNA approaches can elucidate mechanisms of vesicant toxicity and potentially identify targets for drug screening. High-throughput siRNA screening is used by the pharmaceutical industry to mechanistically assess gene function and identify therapeutic targets. For these reasons, we have applied high-throughput siRNA screening technology to the problem of SM cutaneous injury. Our siRNA screening efforts have initially focused on SM-induced inflammation in cutaneous injury. Historical microarray data on this injury were mined for targets and pathways implicated in inflammation. From these data, a siRNA library of 2,017 targets was assembled for screening. Primary screening and library deconvolution were performed using HaCaT cells, a p53-mutated immortal human keratinocyte line (Boukamp et al. 1988). Cells were transfected with siRNA prior to exposure to SM, and the effects on cytokine production and cell viability were analyzed. Using this in vitro approach, we have identified and validated novel targets that regulate SM-induced inflammation that may potentially be useful for the treatment of SM-induced cutaneous inflammation.

Materials and methods

Cell culture

HaCaT cells, a p53-mutated immortal human keratinocyte line, were a kind gift from Dr. John Schlager. These cells were selected for study because they are a human model and have been historically used to study SM in vitro. HaCaT cells were grown in Dulbecco's modified Eagle medium (DMEM) (Life Technologies, Grand Island, NY) supplemented with 10 % fetal bovine serum and 1 % L-glutamine (Life Technologies). Cells were incubated at 37 °C with 5 % CO_2, maintained in 75-cm^2 cell culture flasks, and grown to 70–80 % confluency before trypsin detachment and reseeding at 2.5 × 10^3 cells/cm^2. For primary screening and library deconvolution, cells were trypsinized and seeded into 96-well plates at 3,000 cells/well using a HydraDT 96 channel pipetting robot fitted with an XYZ stage (ThermoFisher, Chicago, IL). For siRNA validation, cells were seeded into 6-well plates at 50,000 cells/well using a standard laboratory pipette.

siRNA and transfection

Dharmacon siGENOME SmartPool siRNA was used for primary screening and Dharmacon ON-TARGETplus siRNA was used for library deconvolution and target validations that utilized siRNA. Lipofectamine RNAiMAX transfection reagent (Life Technologies) was used to transfect the siRNA. For screening and deconvolution, the siRNA libraries were reconstituted, and transfection mixes were prepared and added to cells using a ThermoFisher HydraDT 96 channel pipetting robot. For target validation, siRNA was purchased in tube format. After reconstitution of the siRNA, transfection mixes were prepared and added to cells using standard single channel digital laboratory pipettes. All siRNA was reconstituted with Thermo Scientific 5X siRNA buffer. siRNA and transfection reagent dilutions for transfection were prepared with Opti-MEM-reduced serum medium (Life Technologies). Transfections were performed 1 day after cell seeding. Cells were transfected for 6 h, washed with phosphate-buffered saline (PBS, 10 mM sodium phosphate, 0.9 % NaCl, pH 7.4), and overlaid with fresh DMEM culture medium supplemented with 1 % Penicillin/Streptomycin solution (Sciencell, Carlsbad, CA). Cells were fed the next day with antibiotic-free DMEM, and exposures were performed the following day. This provided a two-day post-transfection time period prior to experimentation to allow for maximum target knockdown. For primary screening and deconvolution, each siRNA was transfected in six replicate wells on six different plates. Three replicate plates were used for SM exposures, and three were unexposed controls. Controls on each 96-well plate included non-targeting siRNA, two toxic siRNAs [siTOX and

siRNA targeting Kif 11 (Dharmacon), positive control p38α Validated Stealth RNAi (Life Technologies)], OptiMEM transfection diluent, and naïve cells. Because siRNA validation studies were performed in 6-well plates, controls were on plates separate from the experimental siRNAs and included non-targeting siRNA, positive control p38α Validated Stealth RNAi, and naïve cells.

In situ mRNA quantitation and high-content analysis

Transfection conditions for individual targets were optimized following deconvolution of the library using the Quantigene View assay (Affymetrix, Santa Clara, CA) to assess gene expression levels. The assay was performed according to the manufacturer's instructions. Briefly, cells were fixed using a 2 % formaldehyde solution. Cells were then permeabilized and digested with the included protease solution diluted 1:1,000 before hybridization of the probe sets. The signal was then amplified and the nuclei counterstained with 1 μg/ml DAPI solution for 3 min. Type 8 target mRNA-specific probe sets with a 550 flurophore were used as well as the Type 8 signal amplification systems. The plate was imaged and analyzed using the Spot Detector Bioapplication on the ArrayScan VTI high-content analyzer (Thermofisher Cellomics Division, Pittsburgh, PA). Using the 20X objective, the XF93-Hoechst and XF93 TRITC filter/dichroic combinations were used to image DAPI and the target mRNA, respectively.

SM exposures

SM was obtained from the US Army Edgewood Chemical Biological Center (Aberdeen Proving Ground, MD). All SM exposures were performed in a certified chemical surety fume hood. A frozen aliquot of neat (undiluted) SM in keratinocyte growth medium was thawed and vortexed to generate 4 mM SM stock solution. This stock solution was placed on ice and immediately diluted into medium to expose cells to SM. The exposure dose was 200 μM SM for all experiments. This dose was selected because it has been historically established to approximate a vesicating dose in skin based on a histopathological comparison of SM-exposed skin and cultured cells. For SM exposures, cells were left at 37 °C with room CO_2 concentrations for a maximum of 30 min and returned to 37 °C with 5 % CO_2. Unexposed controls were also left at 37 °C with room CO_2 concentrations at the same time. Cell viability and expression of cytokines were assessed 24 h after exposure.

Cell viability assay

3-[4,5-dimethylthiazol-2-yl]-2,5-diphenyltetrazolium bromide (MTT) was used to assess cell viability. A stock solution of MTT (Sigma-Aldrich, St. Louis, MO) was made in PBS at 5 mg/ml, filter sterilized, and stored at −20 °C until use. This stock solution was diluted to 0.5 mg/ml in 1X PBS containing 1 mg/ml glucose and pre-warmed to 37 °C. Twenty-four h after SM exposure, the cell culture medium from each well was removed and transferred to 96-well U-bottom plates, sealed, and stored at −80 °C for subsequent analysis. The cells were then overlaid with 100 μl per well of the PBS/glucose/MTT solution and incubated at 37 °C with 5 % CO_2 for 2 h. After incubation, the PBS/glucose/MTT was removed and discarded. The resultant purple formazan, formed by mitochondrial dehydrogenase conversion of MTT, was dissolved by the addition of 100 μl per well isopropanol. The plate was gently shaken on a plate shaker for 1 min, and absorbance at 570 and 690 nm was measured on a SpectraMax M5 plate reader (Molecular Devices, Sunnyvale, CA).

Cytokine analysis

The levels of IL-8 and TNFα in culture medium samples from primary screening and deconvolution were assessed using standard capture ELISA. Antibodies used for the IL-8 ELISA were mouse anti-human IL-8 monoclonal IgG1 clone 6217 (R&D Minneapolis, MN, cat# MAB208) for capture and goat anti-human IL-8 polyclonal (Sigma, St. Louis, MO cat# I8026) for detection. Antibodies used for the TNFα ELISA were mouse anti-human TNFα monoclonal IgG1 clone 28401 (R&D cat# MAB610) for capture and goat anti-human TNFα polyclonal (R&D cat# AF-210-NA) for detection. Both assays used the same rabbit anti-goat IgG (whole molecule) peroxidase-conjugated antibody (Sigma cat# A4174) for labeling. Capture antibody was diluted in PBS, added to Grenier high-binding white 96-well plates, and incubated overnight at 4 °C. The plates were then blocked for 2 h at room temperature with a 50:50 mixture of SuperBlock (Thermo Scientific) and 5 % BSA PBS with 0.5 % Tween 20. The plates were washed five times, samples were added, and then, the plates were incubated for 1 h at room temperature. Detection and labeling antibodies diluted in blocking buffer were added after washing five times and incubated for 1 h each at room temperature. Chemiluminescent Peroxidase Substrate for ELISA (Sigma) was added after a final wash step, and signal was detected using a Spectramax M5 (auto PMT and 500 ms integration time).

For target validation, multiplex analysis of IL-6, IL-8, and TNFα in culture medium samples was performed using a bead-based multiplex cytokine assay (Milliplex, Millipore, Billerica, MA) and analyzed using a Bio-Plex System array reader with Bio-Plex Manager 4.0 software (Bio-Rad Laboratories, Hercules, CA). The data were expressed as the average of three replicates ± standard deviation (SD)

over time ($n = 3$). Data were normalized to the exposed p38α control group averaged across all validation assays and expressed as fold expression relative to this control group. Data were analyzed for statistical significance using a one-way analysis of variance (ANOVA) followed by Dunnett's multiple comparison tests comparing the exposed negative siRNA pool control group that was averaged across all validation assays to all other groups. Statistical significance was defined as $p < 0.05$ for all tests.

Results

Primary screening

Prior to screening, transfection optimization studies were performed using siRNA targeting cyclophilin b to establish transfection conditions necessary to achieve at least 70 % knockdown. Cyclophilin b mRNA levels were measured in situ using the Quantigene View assay (Affymetrix, Santa Clara, CA), and the results quantified by high-content analysis (HCA) using the ArrayScan VTI high-content analyzer (Thermofisher, Cellomics Division, Pittsburgh, PA). We were able to achieve upwards of 90 % knockdown of cyclophilin b with as little as 1.2 pmol of siRNA per well (data not shown). However, we elected to use 10 pmol per well for the primary screening and library deconvolution in order to capture potential targets that might require higher levels of siRNA for effective knockdown. Target knockdown kinetics were also evaluated, and target knockdown was maximal at 2 days after transfection (data not shown). All transfections were performed using plate pipetting robotics, and consistency of knockdown across the plate was validated. Historical microarray data from SM exposures of normal human epidermal keratinocytes (NHEK) and the mouse ear vesicant model (MEVM) were analyzed using Ingenuity Pathway Analysis (IPA) for molecules and pathways implicated in the inflammatory response to SM. This analysis identified 2,017 molecules which were selected as targets for our siRNA library for primary screening. This library was screened in HaCaT cells, and the endpoints assessed were the IL-8 levels by capture ELISA and cell viability by MTT assay. A positive control, siRNA targeting p38α (MAPK13), was included on every plate and was used for data normalization across the study. Though not a focus of the current screening effort, the effect of siRNA on cell viability was also assessed, and the results are shown in Fig. 1. The range of the cell viabilities for all SM-exposed samples was 0.95–52.3 %, and the average cell viability for all SM-exposed samples was 8.71 % (SD = 6.41). Interestingly, six targets improved cell viability to greater than 35 %. These targets are CACNA1B (52.3 %), ALOX5 (40.9 %), CD2AP (40.4 %), CAMK1D (39.1 %), CD247 (37.5 %), and CCR4 (37.2 %) (collectively, the SD of these six targets is 12.3). There is a 6 % gap in cell viability between CCR4 and the next gene, LOC441108; no other performance gap of more than 1 % exists between the remaining targets.

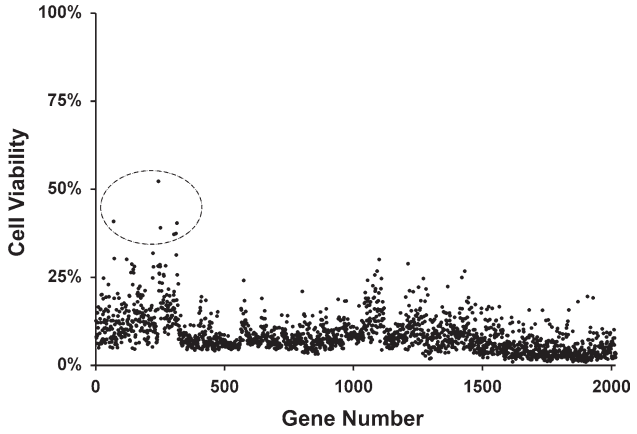

Fig. 1 siRNA Effect on Cell Viability of SM-Exposed HaCaT Cells. Cells were transfected with siRNA for 48 h and then exposed to 200 μM SM. Cell viability was assessed by MTT assay 24 h after exposure. Six targets are circled (CACNA1B, ALOX5, CD2AP, CAMK1D, CD247, and CCR4) that show improved cell viability fourfold to sixfold over the library average of 8.71 %. Results shown are the average of three replicates ($n = 3$)

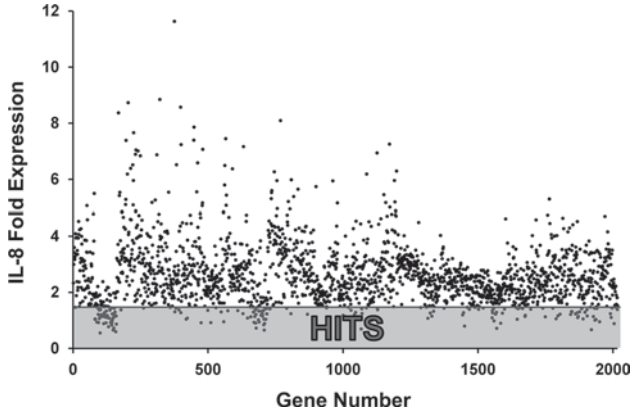

Fig. 2 siRNA Inhibition of IL-8 Production by SM-Exposed HaCaT Cells. Cells were transfected with siRNA for 48 h and then exposed to 200 μM SM. IL-8 in cell culture supernatant was assessed by capture ELISA24 h after exposure. *Shaded area* shows hits within the selection metric of 1.5-fold the positive control. Results shown are the average of three replicates ($n = 3$)

Figure 2 shows the p38α-normalized IL-8 production for each target in the primary screen. A hit selection metric of 1.5-fold the level of IL-8 in SM-exposed p38α-positive controls was chosen as the threshold for selection of target for deconvolution, the next phase of screening. There were 150 targets that met this threshold. The 150 targets selected for deconvolution were mapped using IPA. The significance of the association between the data set and

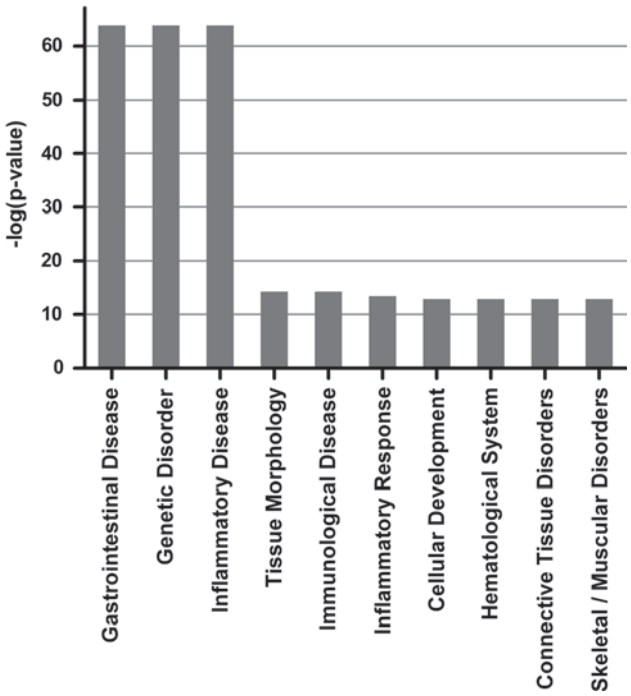

Fig. 3 Top Ten Canonical Pathways by Ingenuity Pathway Analysis

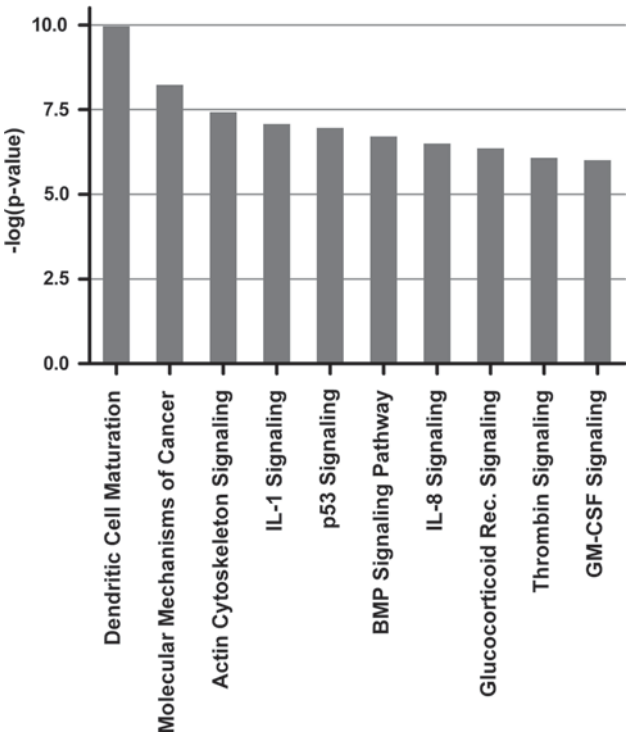

Fig. 4 Top Ten Biological Pathways by Ingenuity Pathway Analysis

the pathway was measured in two ways: (1) A ratio of the number of genes from the data set that map to the pathway divided by the total number of genes that map to the canonical pathway is displayed (Fig. 3): (2) Fisher's exact test was used to calculate a *p* value determining the probability that the association between the genes in the data set and the canonical pathway is explained by chance alone. A negative log value of 1.3 [1.3 = –log (0.05)] was set as being statistically significant. The top ten canonical pathways are shown in Fig. 3. Most of the canonical pathways identified are related to inflammation, which is to be expected given that the library was focused on inflammation by IPA analysis of microarray data. The top three biological pathways, gastrointestinal disease, genetic disorder, and inflammatory disease, all share the same two disorders, inflammatory bowel disease (IBD) [–log (*p* value) = 64.1] and Crohn's disease [–log (*p* value) = 59.4] (Fig. 4).

Deconvolution

Because the primary screening phase utilized four pooled siRNA sequences to knockdown each target, hits from the primary screen underwent deconvolution in which each of the siRNA sequences was evaluated separately. As stated previously, 150 targets met the hit selection threshold in primary screening, and 72 targets have been deconvoluted thus far. Deconvolution was performed with HaCaT cells, and the end points assessed by capture ELISA were IL-8 and TNFα. Only two cytokines were selected for end points in deconvolution in order to simplify the screening process. IL-8 and TNFα were selected over IL-6 because they are more broadly implicated in overall cornea health, whereas IL-6 has been more frequently implicated in a specific cornea pathology, neovascularization. Cell viability was assessed by MTT assay. All the same controls used for primary screening were used for deconvolution. Cytokine data were normalized to the p38α-positive control, and results are shown in Fig. 5. The normalized IL-8 expression for most of the sequences (323/600) was less than 1.5, and for TNFα, many (298/600) were <1. There were several considerations for hit selection in deconvolution. A primary factor was that three or four out of four sequences demonstrated cytokine knockdown less than or equal to one for both the IL-8 and the combined scores. Other factors considered were known roles for the target and likelihood that the target was "druggable." For example, little is known about the roles of CORIN and ZNF547 in cellular physiology, and these were selected for further study. Much is known about the roles of MAPKs and RELA in cells and attempts to develop drugs for some of them have been largely unsuccessful; therefore, these were excluded from study.

siRNA target validation

Twelve targets were selected from deconvolution for in vitro validation: BAZB1, CLSTN2, CORIN, DMBT1,

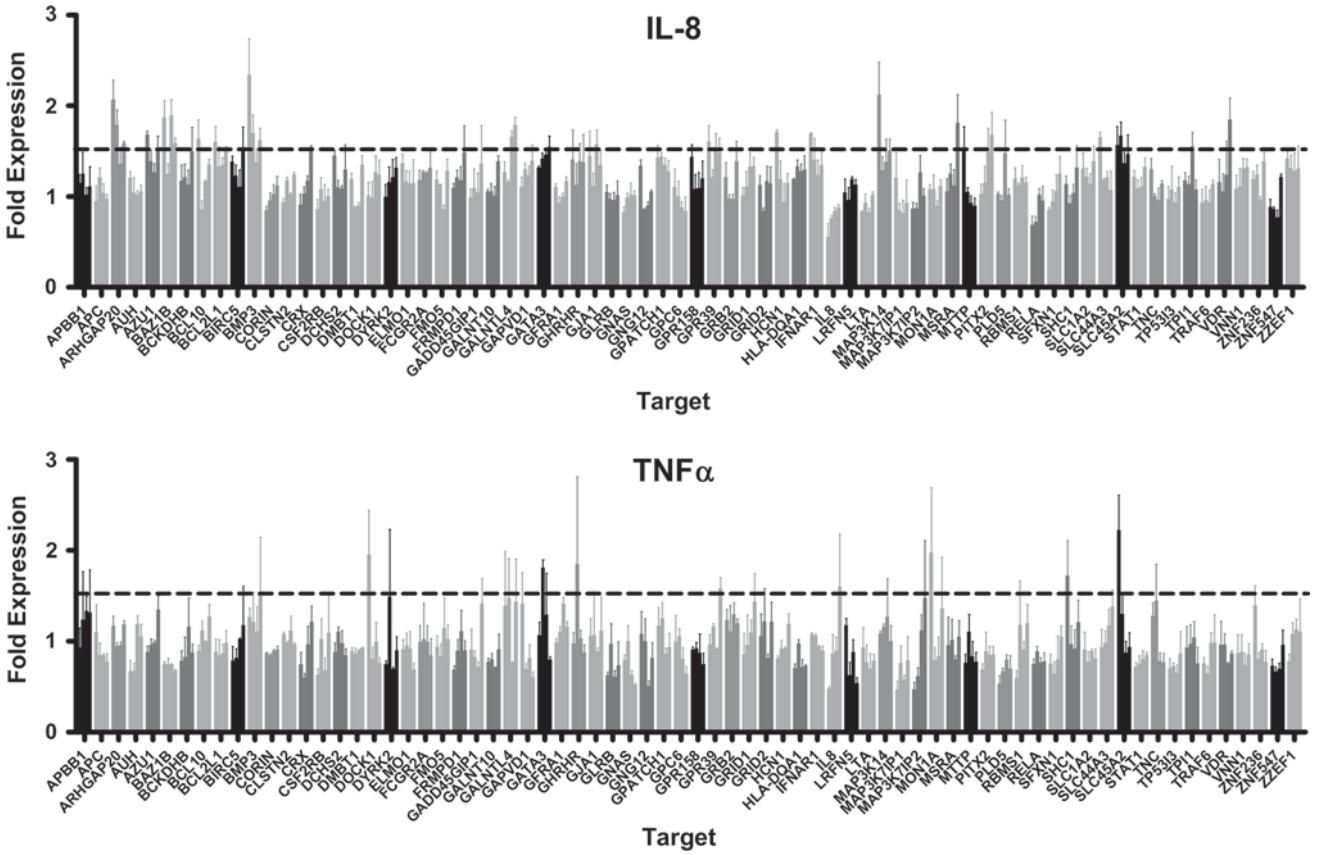

Fig. 5 siRNA Inhibition of IL-8 and TNFα Production by SM-Exposed HaCaT Cells in Library Deconvolution. Cells were transfected with siRNA for 48 h and then exposed to 200 μM SM. IL-8 and TNFα in cell culture supernatant were assessed by capture ELISA assay 24 h after exposure. Results shown are the average of three replicates ± SE ($n = 3$). *Dotted line* shows performance of the p38α positive control

GALNT10, GFRA1, GNAS, HCN1, HLA-DQA1, IFNAR1, TRAF6, and ZNF547. The two sequences for each target with the best inhibition of cytokine production from deconvolution were selected for use in validation studies. Transfection was optimized for each siRNA sequence studied using the Quantigene View assay as previously described. End points were cell viability by MTT and multiplex assessment of IL-6, IL-8, and TNFα by Milliplex bead-based cytokine assay. The two siRNA sequences for each target were tested separately and in combination. When tested in combination, the total amount of siRNA was kept equal to that of separately tested sequences. Experimental groups for which both sequences and the combination of sequences significantly inhibited cytokine production are marked with an asterisk (Fig. 6). There were several experimental groups for IL-6 and IL-8 that had statistically significant cytokine inhibition relative to the exposed negative pool control group. The actual decrease in cytokine production was marginal, but the data were significant owing to the small standard error. Only CORIN significantly inhibited cytokine production to less than half of the negative pool control group for all three cytokines evaluated. For IL-6, GNAS was also able to reduce cytokine production to less than half of the negative pool control group.

Discussion

Herein, we report on work thus far on a high-throughput siRNA screening paradigm to understand the molecular mechanisms of vesicant injury and identify potential targets for the treatment of this injury. The siRNA library we utilized was focused on inflammatory pathways because chronic inflammation after exposure appears to play a role in progressive clinical pathology and intervention may improve clinical outcome. The end points selected for this screen, inflammatory cytokine production and cell viability, were selected because targets that mitigate cellular injury should reduce SM-induced cell death and inflammation.

Our results demonstrate that knockdown of GNAS significantly inhibited SM-induced IL-6 production and knockdown of CORIN significantly inhibited SM-induced

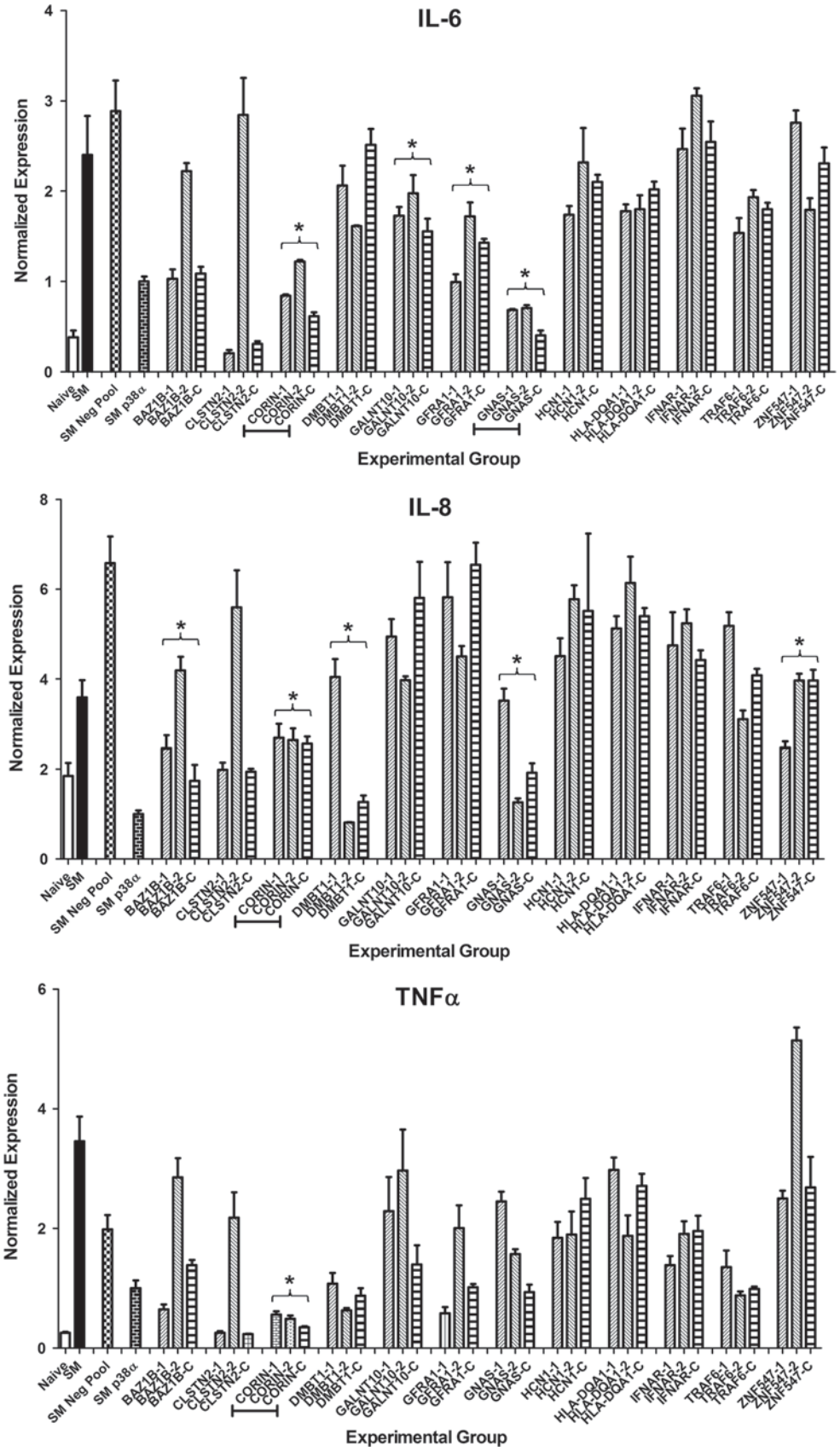

Fig. 6 siRNA Inhibition of IL-6, IL-8, and TNFα Production by SM-Exposed HaCaT Cells in Target Validation. Cells were transfected with siRNA for 48 h, and then exposed to 200 μM SM. Two siRNA sequences for each target were tested under sequence-specific optimized transfection conditions. Each sequence was tested separately (labeled as −1 and −2) and in combination (labeled as −C). Cytokines in cell culture supernatant were assessed 24 h after exposure by multiplex assay. Results shown are the average of three replicates ± SE ($n = 3$). The results for the control groups Naïve, SM, SM Neg Pool, and SM p38α are provided for reference. Targets for which both sequences and the combination of sequences had cytokine production significantly less than the SM-exposed negative pool control group are indicated by *asterisks* ($*p < 0.05$). CORIN and GNAS (*underlined*) inhibited cytokine production to less than half the SM-exposed negative pool control group

IL-6, IL-8, and TNFα production. The finding that CORIN knockdown inhibited production of all three cytokines, but that GNAS knockdown inhibited production of only IL-6 suggests that GNAS may be downstream of CORIN in the regulation of these cytokines in SM cutaneous injury. GNAS is a complex locus which produces many transcripts. Gs-alpha is perhaps the most well-characterized transcript, and it encodes the alpha subunit of stimulatory guanine nucleotide-binding proteins (G protein). G proteins play a wide variety of physiologic roles and are expressed in almost all cells and tissues. With regard to inflammation, Gα12 has been shown to regulate both IL-6 and IL-8 in oral squamous cell carcinoma (Jian et al. 2013). CORIN is a serine protease that converts pro-atrial natriuretic peptide (pro-ANP) to biologically active ANP, which plays a role in the regulation of blood pressure (Wu et al. 2009). Little is known regarding other potential roles for this molecule. However, recently, it has been shown to be up-regulated in the deciduas of the pregnant uterus, and CORIN gene mutations have been associated with preeclampsia, suggesting a role for CORIN in pregnancy (Zhou and Wu 2013). Although our identification of a role for CORIN in SM-induced cutaneous inflammation is distinctive from any previously identified role for this molecule, it is consistent with its biochemical activity, as there are a number of serine proteases that play a role in regulating the immune system and inflammation (Safavi and Rostami 2012).

Although our siRNA library was focused on inflammatory pathways, we identified six targets that increased cell viability fourfold to sixfold over the average cell death for the entire screen. Knockdown of CACNA1B (the alpha-1B subunit of calcium channel) or CAMK1D (calcium/calmodulin-dependent protein kinase 1-delta) improved cell viability following SM exposure. These findings are consistent with the known role of calcium signaling in SM-induced cell death and differentiation (Rosenthal et al. 2000). ALOX5 is a lipoxygenase that has a role in the catalysis of leukotrienes. Although prostaglandin and leukotriene synthases have been shown to have a role in SM inflammation (Black et al. 2010; Tanaka et al. 1997), this is the first data to demonstrate a potential role of leukotrienes in SM-induced cell death. Interestingly, three of the knockdown targets that improved cell viability have known roles in T-cell physiology: (1) CD247, the zeta chain of the T-cell antigen receptor; (2) CCR4, a CC chemokine receptor; and (3) CD2AP, a multifunctional adapter-type scaffolding protein involved in the regulation of the actin cytoskeleton. This finding is curious given that our studies were conducted with HaCaT cells, which are not known to have any contaminating immune cells or to express T-cell-related molecules. It is important to note that these were initial findings from primary screening, and the role of these targets in SM cell viability has not been validated. It is also important to restate that primary screening was performed using Dharmacon siGENOME siRNA, which can have greater off-target effects relative to Dharmacon ON-TARGETplus, which was used for target validation. Further studies are necessary to validate the roles of these molecules in SM-induced cell death, and in the case of CD247, CCR4, and CD2AP, future studies should confirm if in fact HaCaT cells and primary keratinocytes express these proteins.

The top ten canonical pathways identified by pathway mapping were largely related to immune function, which is to be expected given the focus of our siRNA library on inflammation. It is interesting to note that p53 signaling and molecular mechanisms of cancer were two of the top ten pathways. While this is consistent with the radiomimetic properties of SM, any potential role for p53 or DNA damage in SM-induced inflammation remains unclear at this time. The top three biological pathways are all related by IBD and Crohn's disease. TNFα is a major regulator of these disorders, and TNFα was shown to be the most highly interconnected molecule in the pathway mapping analysis of our deconvolution library (data not shown). This suggests a similarity between SM cutaneous injury and IBD/Crohn's disease at least in regard to an important role for TNFα in SM injury. TNFα blockade is an effective clinical strategy for the management of IBD and Crohn's disease. Although TNFα blockade alone is not effective in treating SM cutaneous injury, Etanercept (a soluble TNFα receptor) is a necessary component of a combinatorial therapy that has shown some modest efficacy in treating this injury (personal communication, James Dillman, PhD).

We did not identify an effect on IL-1β, which is commonly up-regulated in cellular injury, because SM-injured HaCaT cells do not produce this cytokine in our laboratory. Future work will investigate any effect on IL-1β production using primary keratinocytes, which do express IL-1β in SM injury. Although we have many more targets for which the down selection and validation process has yet to be completed, we have identified that CORIN regulates the cytokines IL-6, IL-8, and TNFα in cutaneous SM injury. A role for CORIN in vivo remains to be validated, and the known role of CORIN in regulating blood pressure presents important considerations for its clinical potential as a therapeutic target for SM. However, we believe this finding validates our approach that high-throughput siRNA screening can identify potential therapeutic targets for chemical injury. Further studies are necessary to validate the roles of other targets in SM inflammation, and additional siRNA libraries, such as those focused on cell death pathways, should be screened in future efforts to investigate other mechanisms.

Acknowledgments This research was supported by the Defense Threat Reduction Agency—Joint Science and Technology Office, Medical S&T Division, Project ID Number CBM.CUTOC.04.10. RC.001.

Conflict of interest None.

References

Black AT, Hayden PJ, Casillas RP et al (2010) Expression of proliferative and inflammatory markers in a full-thickness human skin equivalent following exposure to the model sulfur mustard vesicant, 2-chloroethyl ethyl sulfide. Toxicol Appl Pharmacol 249(2):178–187. doi:10.1016/j.taap.2010.09.005

Boukamp P, Petrussevska RT, Breitkreutz D, Hornung J, Markham A, Fusenig NE (1988) Normal keratinization in a spontaneously immortalized aneuploid human keratinocyte cell line. J Cell Biol 106(3):761–771

Deaton MA, Jones GP, Bowman PD (1990) [14C]mechlorethamine binding to proteins of the human keratinocyte. Mil Med 155(10):477–480

Dillman JF 3rd, McGary KL, Schlager JJ (2003) Sulfur mustard induces the formation of keratin aggregates in human epidermal keratinocytes. Toxicol Appl Pharmacol 193(2):228–236

Dillman JF 3rd, Hege AI, Phillips CS et al (2006) Microarray analysis of mouse ear tissue exposed to bis-(2-chloroethyl) sulfide: gene expression profiles correlate with treatment efficacy and an established clinical endpoint. J Pharmacol Exp Ther 317(1):76–87

Fox M, Scott D (1980) The genetic toxicity of nitrogen and sulphur mustard. Mutat Res 75:131–168

Herriott RM, Price WH (1948) The formation of bacterial viruses in bacteria rendered non-viable by mustard gas. J Gen Physiol 32(1):63–68

Jian SL, Hsieh HY, Liao CT et al (2013) Galpha(1)(2) drives invasion of oral squamous cell carcinoma through up-regulation of proinflammatory cytokines. PLoS One 8(6):e66133

Kehe K, Balszuweit F, Steinritz D, Thiermann H (2009) Molecular toxicology of sulfur mustard-induced cutaneous inflammation and blistering. Toxicology 263(1):12–19

Langenberg JP, van der Schans GP, Spruit HE et al (1998) Toxicokinetics of sulfur mustard and its DNA-adducts in the hairless guinea pig. Drug Chem Toxicol 21(Suppl 1):131–147

Lawley PD, Brookes P (1965) Molecular mechanism of the cytotoxic action of difunctional alkylating agents and of resistance to this action. Nature 206:480–483

Lawley PD, Brookes P (1968) Cytotoxicity of alkylating agents towards sensitive and resistant strains of Escherica coli in relation to extent and mode of alkylation of cellular macromolecules and repair of alkylation lesions in deoxyribonucleic acids. Biochem J 109:433–447

Papirmeister B, Westling AW, Schroer J (1969) Mustard: The relevance of DNA damage to the development of the skin lesion., vol DTIC No. AD-688-866. U.S. Army Medical Research Laboratory, Edgewood Arsenal

Papirmeister B, Feister A, Robinson S, Ford R (1991) Medical defense against mustard gas: toxic mechanisms and pharmacological implications. CRC Press, Boca Raton

Popp T, Egea V, Kehe K et al (2011) Sulfur mustard induces differentiation in human primary keratinocytes: opposite roles of p38 and ERK1/2 MAPK. Toxicol Lett 204(1):43–51. doi:10.1016/j.toxlet.2011.04.007

Rogers JV, Choi YW, Kiser RC et al (2004) Microarray analysis of gene expression in murine skin exposed to sulfur mustard. J Biochem Mol Toxicol 18(6):289–299

Rosenthal DS, Simbulan-Rosenthal CM, Iyer S, Smith WJ, Ray R, Smulson ME (2000) Calmodulin, poly(ADP-ribose)polymerase and p53 are targets for modulating the effects of sulfur mustard. J Appl Toxicol 20(Suppl 1):S43–S49

Ruff AL, Dillman JF (2007) Signaling molecules in sulfur mustard-induced cutaneous injury. Eplasty 8:e2

Ruff AL, Dillman JF 3rd (2010) Sulfur mustard induced cytokine production and cell death: investigating the potential roles of the p38, p53, and NF-kappaB signaling pathways with RNA interference. J Biochem Mol Toxicol 24(3):155–164. doi:10.1002/jbt.20321

Sabourin CL, Rogers JV, Choi YW et al (2004) Time- and dose-dependent analysis of gene expression using microarrays in sulfur mustard-exposed mice. J Biochem Mol Toxicol 18(6):300–312

Safavi F, Rostami A (2012) Role of serine proteases in inflammation: Bowman–Birk protease inhibitor (BBI) as a potential therapy for autoimmune diseases. Exp Mol Pathol 93(3):428–433

Tanaka F, Dannenberg AM Jr, Higuchi K et al (1997) Chemotactic factors released in culture by intact developing and healing skin lesions produced in rabbits by the irritant sulfur mustard. Inflammation 21(2):251–267

Wu Q, Xu-Cai YO, Chen S, Wang W (2009) Corin: new insights into the natriuretic peptide system. Kidney Int 75(2):142–146

Zhou Y, Wu Q (2013) Role of corin and atrial natriuretic peptide in preeclampsia. Placenta 34(2):89–94